

Journal Pre-proof

Constructing $\text{Pt}^{\text{I}}@ \text{COF}$ for semi-hydrogenation reactions of phenylacetylene

Jian Hong Li, Zhi Wu Yu, Jian Qiang Li, Ya Ling Fan, Zhi Gao, Jian Bo Xiong, Li Wang, Yuan Tao, Li Xiao Yang, Yu Xin Xiao, Feng Luo



PII: S0022-4596(20)30006-2

DOI: <https://doi.org/10.1016/j.jssc.2020.121176>

Reference: YJSSC 121176

To appear in: *Journal of Solid State Chemistry*

Received Date: 17 December 2019

Revised Date: 2 January 2020

Accepted Date: 4 January 2020

Please cite this article as: J.H. Li, Z.W. Yu, J.Q. Li, Y.L. Fan, Z. Gao, J.B. Xiong, L. Wang, Y. Tao, L.X. Yang, Y.X. Xiao, F. Luo, Constructing $\text{Pt}^{\text{I}}@ \text{COF}$ for semi-hydrogenation reactions of phenylacetylene, *Journal of Solid State Chemistry* (2020), doi: <https://doi.org/10.1016/j.jssc.2020.121176>.

This is a PDF file of an article that has undergone enhancements after acceptance, such as the addition of a cover page and metadata, and formatting for readability, but it is not yet the definitive version of record. This version will undergo additional copyediting, typesetting and review before it is published in its final form, but we are providing this version to give early visibility of the article. Please note that, during the production process, errors may be discovered which could affect the content, and all legal disclaimers that apply to the journal pertain.

© 2020 Published by Elsevier Inc.

Feng Luo: Conceptualization, Methodology, Software

Jian Hong Li: Data curation, Writing- Original draft preparation.

Ya Ling Fan, Yuan Tao, Li Xiao Yang: Visualization, Investigation.

Yu Xin Xiao: Supervision.:

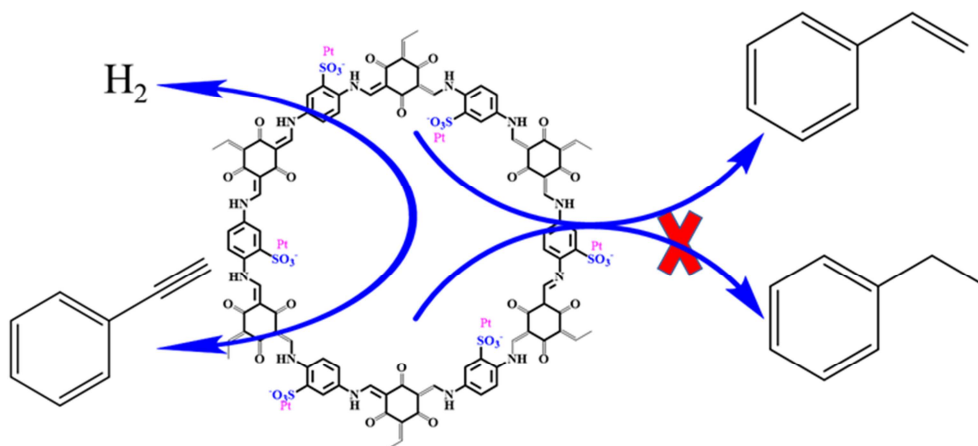
Zhi Wu Yu, Jian Qiang Li, Jian Bo Xiong: Software, Validation.:

Zhi Gao, Li Wang: Writing- Reviewing and Editing,

,

Constructing Pt^I@COF for Semi-Hydrogenation Reactions of Phenylacetylene

Jian Hong Li^{ab, †}, Zhi Wu Yu^{c, †}, Jian Qiang Li^a, Ya Ling Fan^a, Zhi Gao^a, Jian Bo Xiong^a, Li Wang^a, Yuan Tao^a, Li Xiao Yang^a, Yu Xin Xiao^a and Feng Luo^{a*}



A noble catalyst Pt[□]@COF was first prepared, which exhibits remarkable performance for semi-hydrogenation of phenylacetylene, including high selectivity, turnover frequency value, good recycle, strong stability.

Constructing Pt^I@COF for Semi-Hydrogenation Reactions of Phenylacetylene

Jian Hong Li^{ab, †}, Zhi Wu Yu^{c, †}, Jian Qiang Li^a, Ya Ling Fan^a, Zhi Gao^a, Jian Bo Xiong^a, Li Wang^a, Yuan Tao^a, Li Xiao Yang^a, Yu Xin Xiao^a and Feng Luo^{a*}

^aState Key Laboratory for Nuclear Resources and Environment, and School of Biology, Chemistry and Material Science, East China University of Technology, Nanchang, Jiangxi 344000, China,

^bChina Institute of Atomic Energy, Beijing 102413, China

^cHigh Magnetic Field Laboratory, Chinese Academy of Sciences, Hefei 230031, Anhui, P. R. China

[†]These authors are the co-first author.

* Corresponding author. E-mail address: ecitluofeng@163.com (F. Luo).

Abstract: The great efforts have been devoted to fabricate excellent hydrogenation catalysts owing to the broad applications in industrial fields. However, the preparation processes of traditional hydrogenation catalysts are often complicated. Herein, mono-valence Pt^I@COF was synthesized as a catalyst for semi-hydrogenation of phenylacetylene for the first time. The easily prepared SO₃H-linked COF possesses a two-dimensional eclipsed layered-sheet structure, making its incorporation with metal ions feasible. The as-prepared Pt^I@COF composite exhibits excellent performance for semi-hydrogenation phenylacetylene with 93.5% conversion and 90.2% selectivity to styrene under mild reaction conditions (1 bar H₂, 25°C) within 20 min. It's worth noting that the turnover frequency (TOF) value reaches at 3965 h⁻¹, which outperforms most of recently reported excellent Pt-based catalysts for this reaction.

1 **Keywords:** hydrogenation catalysts; Pt^I@COF; turnover frequency; mono-valence.

2 **1. Introduction**

3 As a harmful material in polymerization of styrene, phenylacetylene readily results in catalyst
4 poisoning during styrene polymerization and thus affects properties of polystyrene. In this sense,
5 removing phenylacetylene *via* selective hydrogenation process is necessary for improving
6 qualities of polymerized styrene materials. [1-3] However, the selectivity to the desired styrene is
7 usually unsatisfied because of the easy generation of over-hydrogenation product
8 phenylethane. [4-5] Up to now, intensive research endeavors have been devoted to develop excellent
9 catalysts for selective hydrogenation of phenylacetylene to styrene. It was found that noble metal
10 (Pt, Pd, Au etc.) catalysts are the ideal choice because of their high catalytic activity and durable
11 stability. [6-10] Amongst Pd-based materials are used intensively in the hydrogenation of
12 phenylacetylene because of their strong dissociative ability for H₂. [11] However, some shortcomings,
13 such as unsatisfied catalytic selectivity, high metal content and long reaction time, hinder their
14 industrial applications. [12-25] Thus, developing new catalysts for efficiently catalyzed
15 hydrogenation of phenylacetylene is urgent.

16 To date, Pt-based catalysts loaded on different supports including carbon nanotubes, [26-27]
17 triphenylphosphine polymer, [28] resin, [29] zeolite-templated carbon [20] were investigated for
18 semi-hydrogenation of phenylacetylene. For example, Li *et al.* reported a CNT-supported Pt
19 catalyst (Pt/CNTs) for hydrogenation of phenylacetylene, where the conversion and the selectivity
20 of styrene can reach at 98% and 86%, respectively.¹⁷ Pt/PSiO₂ catalyst reported by Fukuoka *et al.*
21 exhibited 99.1% conversion of phenylacetylene and 99.5% selectivity to styrene. [30] Nevertheless,
22 the low intrinsic activity (TOF value) of these catalysts stimulate us to design new catalysts. For

aforementioned Pt-based catalysts, their catalytic activities were realized by reduction of the Pt^{2+} species to zero valence Pt (Pt^0), which endowed the metal active site for catalysis. In contrast to the zero-valence state Pt^0 , mono-valence Pt^{I} metal composite, which may improve the intrical activity of Pt-based catalysts, has not been studied for catalyzing hydrogenation of phenylacetylene ever.

In recent years, covalent organic frameworks (COFs) have attracted considerable interest since the first discovery by Yaghi and co-workers in 2005,[31] which comprised of periodically extended and covalently bound crystalline porous network structures.[32] Our group has synthesized a novel material named COF-SO₃H for uranium extraction from sea water, in which the COF-SO₃H can bear strong acid and alkali.[33-34] Thus, we believe that COF-SO₃H should be excellent support to prepare Pt-based catalysts, which are not well investigated in heterogeneous catalysis.

Herein, an ammonium-modified material of $[\text{NH}_4]^+ [\text{COF-SO}_3^-]$ as a support to load Pt nanoparticles for semi-hydrogenation of phenylacetylene was studied. Apart from stabilizing Pt nanoparticles, the $[\text{NH}_4]^+ [\text{COF-SO}_3^-]$ can also form strong chelates with Pt^+ and thus enhances the activity.[35]

2. Experimental section

2.1 Synthesis of catalysts

2.1.1 Synthesis of 1,3,5-triformylphloroglucinol

The ligand material 1,3,5-triformylphloroglucinol was synthesized in the light of the reported literature.[36] Firstly, the hexamethylenetetramine (15.098g, 108mmol) and dried phloroglucinol (6.014g, 49mmol) were added in a three-necked round-bottomed flask with 90mL trifluoroacetic acid. Then the mixture solution was stirred for 2h at 100°C under N₂ condition in oil bath pan. 150mL 3mol/L HCl was added in the flask and continued to stir 2h. After that, the mixture solution

was filtered by kieselguhr and extracted with dichloromethane at room temperature. The obtained yellow solution was steamed using rotary evaporation at 50°C and washed with hot ethanol after dried over magnesium sulfate. Finally, the yellow powder was obtained after dried under vacuum.

2.1.2 Synthesis of 2, 5-dihydroxy benzenesulfonate amine

Briefly, 63mg 1,3,5-triformylphloroglucinol and 84.7mg 2, 5-diaminobenzene sulfonic acid, 3mL N-butyl alcohol and 3mL o-dichlorobenzene were added to a 100 mL Schlenk tube in order. After that the turbid solution was flash frozen in liquid nitrogen for three times after added acetic acid(0.5mL,3mol/L). In the end, the tube was put into the muffle and set the temperature slowly raised to 120 at 10□/min. The reaction was kept 120°C for 3 days and cooled to room temperature at 6°C/h. Crimson powders were obtained by centrifugation with acetone and dried under vacuum.

2.1.3 Synthesis of $[\text{NH}_4]^+[\text{COF-SO}_3^-]$

The ion-exchange material of $[\text{NH}_4]^+[\text{COF-SO}_3^-]$ is obtained by immersing $\text{COF-SO}_3\text{H}$ in $\text{NH}_3\cdot\text{H}_2\text{O}$ (1%) for 24 h and washed by water and methanol. Crimson powders were obtained by centrifugation with acetone and dried under vacuum.

2.1.4 Synthesis of $\text{Pt}^{\text{I}}@\text{COF}$

The catalyst material was synthesized as followed. 100mg $[\text{NH}_4]^+[\text{COF-SO}_3^-]$ is dispersed in 14mL deionized water and then added 400uL 0.125mol/L $[\text{Pt}(\text{NH}_3)_4](\text{NO}_3)_2$ stirring for 2h. After that, the mixture washed by deionized water and methanol and dried at drying oven. Then, the dried power is dispersed in 14mL deionized water and dropwise NaBH_4 (4mL 1mol/L) to reduce for 6 h under N_2 atmosphere. Finally, the crimson power sample was washed and dried at 60°C overnight and marked as $[\text{NH}_4]^+[\text{COF-SO}_3^-]$. The content of Pt in $[\text{NH}_4]^+[\text{COF-SO}_3^-]$ is around 0.83 wt.% confirmed by ICP.

2.1.5 Synthesis of Pt⁰@COF

The prepared Pt⁰@COF was obtained by NaBH₄(4mL 1mol/L) sprayed into [Pt(NH₃)₄](NO₃)₂(400uL 0.125mol/L) solution for stirring at N₂ atmosphere. After that, the 100mg [NH₄]⁺[COF-SO₃⁻] was added and stirring for 2h. Finally, the mixture solution was dried under vacuum oven at 60°C.

2.2 Characterization

The morphologies of the material were obtained by SEM-EDS (scanning electron microscope-Energy Dispersive Spectrometer) measurements using a Hitachi S-4800 microscope. The powder data were collected by PXRD (X-ray powder diffraction) using a Bruker AXS D8 Discover powder diffractometer with monochromatized Cu-K α radiation (at 40 kV, 40 mA, $\lambda = 1.5406\text{\AA}$) in the range of $2\theta = 3-85^\circ$ with a step size of 0.018 and a count time of 5 s per step. The simulated powder patterns were calculated by Mercury 1.4. IR (Infrared Spectra) measurements were measured by a Bruker VERTEX 70 spectrometer in the 500-4000 cm⁻¹ region. X-ray photoelectron spectroscopy (XPS) was conducted using an ESCALAB250 spectrometer. The gas adsorption isotherms were collected on a Belsorp-max. Ultrahigh-purity-grade (>99.999%) N₂ gases were used during the adsorption measurement. The Pt content in catalyst was measured by inductively coupled plasma-mass spectroscopy (ICP-MS, NexION 300X). The catalytic reaction was traced and identified by gas chromatography (GC, Agilent 7890A with a 0.25 mm \times 30 m DB-5 capillary column) using an internal standard technique. Transmission electron microscopy (TEM) micrographs were collected on a FEI Tecnai G2 F20 transmission electron microscope at an accelerating voltage of 200 kV.

2.3 Catalyst test

2.3.1 General Procedure for the Catalytic Hydrogenation of Phenylacetylene

In a typical procedure for catalytic activity test of Pt^I@COF, 114 μ L (1 mmol) of phenylacetylene, 15 mg of catalyst and 15 mL of ethanol as solvent were charged into a three-necked, round-bottomed flask. Afterwards, the flask was purged with 1 MPa H₂ for several minutes to allow pure H₂ atmosphere for the reaction. At this time, the mixture was magnetically stirred at 25 °C temperature and the reaction time was calculated at this point. Samples with 0.5 mL withdrawn at regular intervals of reaction time were analyzed by GC (GC-2014) equipped with an FID detector and a capillary column (DB-5, 30 m 0.45 mm 0.42 mm). The conversion, selectivity and turnover frequency (TOF) were calculated on basis of the following equations:

$$\text{Conversion \%} = \frac{\text{Phenylacetylene feed(mol)} - \text{Phenylacetylene residue(mol)}}{\text{Phenylacetylene feed(mol)}} \times 100\%$$

$$\text{Selectivity \%} = \frac{\text{Styrene product(mol)}}{\text{Phenylacetylene feed(mol)} - \text{Phenylacetylene residue(mol)}} \times 100\%$$

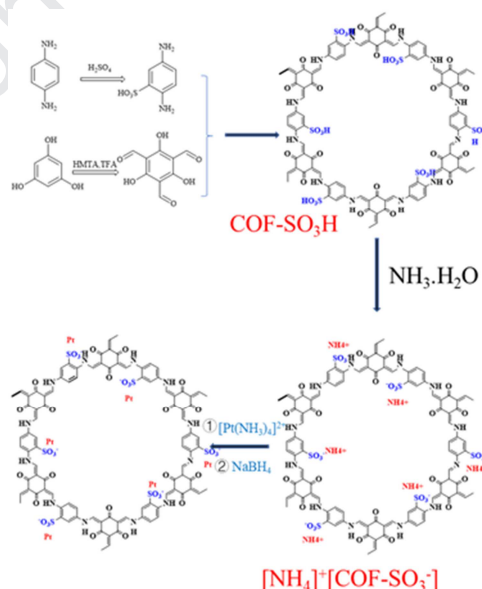
$$\text{TOF(h}^{-1}\text{)} = (\text{n}_{\text{Phenylacetylene}} \times \text{C}_{\text{conversion}} \times \text{C}_{\text{selectivity}}) / \text{n}_{\text{Pt}} \times \text{t}$$

2.3.2 Reuse experiment

In the reuse experiment, the catalyst was isolated by centrifugation and washed with ethanol and dried at 70 °C under vacuum. The same amount of phenylacetylene was added at every catalytic reaction. After every catalytic reaction, the conversion and the selectivity of the products were determined by GC.

3. Results and discussion

As depicted in **scheme 1**, the synthesis of $\text{Pt}^{\text{I}}@\text{COF}$ includes four steps. Firstly, $\text{COF-SO}_3\text{H}$ was prepared through condensation between 1,3,5-triformylphloroglucinol and 2,5-diaminobenzene sulfonic acid by the solvothermal method. Then the $\text{COF-SO}_3\text{H}$ was aminated by $\text{NH}_3\cdot\text{H}_2\text{O}$ to obtain $[\text{NH}_4]^+[\text{COF-SO}_3^-]$. After that, the metal precursor $[\text{Pt}(\text{NH}_3)_4](\text{NO}_3)_2$ solution of Pt^{2+} was deposited in the $[\text{NH}_4]^+[\text{COF-SO}_3^-]$ material by ion exchange. Finally, Pt^{2+} was reduced to Pt^{I} under N_2 atmosphere using NaBH_4 as reducing agent. A series of characterizations were carried out for $\text{COF-SO}_3\text{H}$, $[\text{NH}_4]^+[\text{COF-SO}_3^-]$ and $\text{Pt}^{\text{I}}@\text{COF}$. The powder X-ray diffraction (PXRD) data of $\text{COF-SO}_3\text{H}$ and $[\text{NH}_4]^+[\text{COF-SO}_3^-]$ agree with the simulated one by Material Studio Forcite molecular dynamics method (**Fig. 1a**). ^{13}C CP-MAS solid-state NMR spectroscopy (**Fig. 2**) further proves the β -ketoenamine-linked structure in $\text{COF-SO}_3\text{H}$.^[32] $[\text{NH}_4]^+[\text{COF-SO}_3^-]$ immersed in strong acid, boiling water and strong base was characterized by PXRD testes. The results demonstrate that the $[\text{NH}_4]^+[\text{COF-SO}_3^-]$ possess high chemical stability. (**Fig. 3b**)



Scheme 1. Synthetic scheme of SO_3H -decorated COF ($\text{COF-SO}_3\text{H}$), the ammoniated material of $[\text{NH}_4]^+[\text{COF-SO}_3^-]$ and Pt-loaded material of $\text{Pt}^{\text{I}}@\text{COF}$.

From the PXRD patterns (**Fig. 1b**) of $\text{Pt}^{\text{I}}@\text{COF}$, three intense peaks were found at 40° , 46° and 67° , which were arranged to the (111), (200) and (220) reflections of face-centered cubic (fcc) Pt crystal (JCPDS card, No. 04-0802), indicating the formation of Pt nanoparticles.[32] SEM image revealed that $\text{Pt}^{\text{I}}@\text{COF}$ still can keep the uniform fiber morphology as observed for $\text{COF-SO}_3\text{H}$ and $[\text{NH}_4]^+[\text{COF-SO}_3^-]$. (**Fig. 4**) The character peak of $-\text{C-N}$ ($\sim 1213 \text{ m}^{-1}$) and $-\text{C}=\text{C}$ ($\sim 1567 \text{ cm}^{-1}$) was discovered from the FTIR spectrum of $\text{Pt}^{\text{I}}@\text{COF}$, which almost identical to that of $[\text{NH}_4]^+[\text{COF-SO}_3^-]$. Noteworthy, disappearance of NH_4^+ with hydrogen bonds at 3210 cm^{-1} confirmed the ion exchange between Pt and $[\text{NH}_4]^+$. (**Fig. 5**)

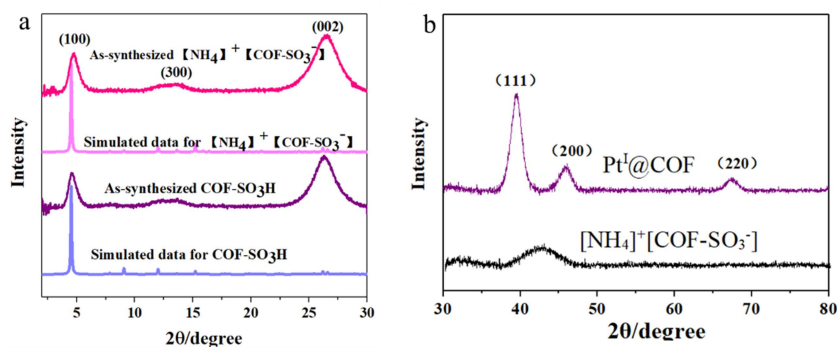


Fig. 1 a) The experimental and calculated PXRD patterns of $\text{COF-SO}_3\text{H}$ and $[\text{NH}_4]^+[\text{COF-SO}_3^-]$. b) XRD patterns of $[\text{NH}_4]^+[\text{COF-SO}_3^-]$ and $\text{Pt}^{\text{I}}@\text{COF}$.

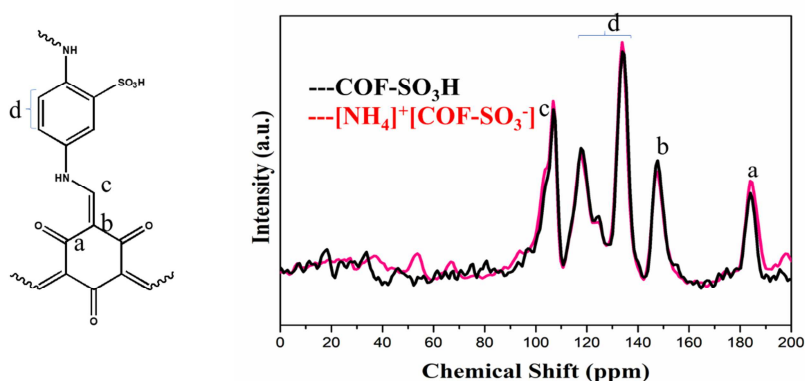


Fig. 2 ^{13}C CP-MAS spectrum of $\text{COF-SO}_3\text{H}$ and $[\text{NH}_4]^+[\text{COF-SO}_3^-]$.

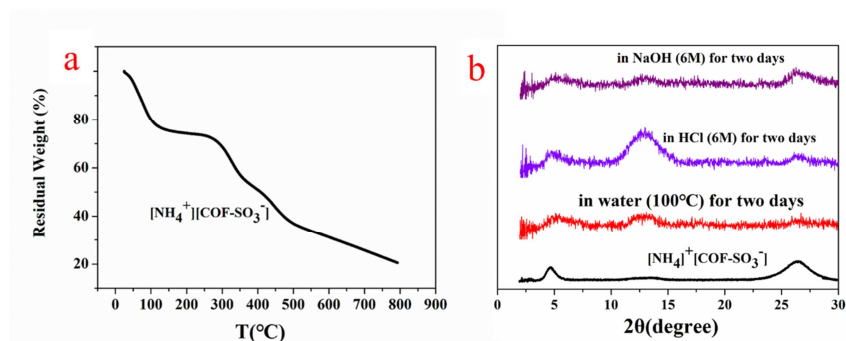


Fig. 3 a) TGA of $[\text{NH}_4^+][\text{COF-SO}_3^-]$, b) The chemostability of $[\text{NH}_4^+][\text{COF-SO}_3^-]$ under boiling water, strong acid and strong base by PXRD patterns.

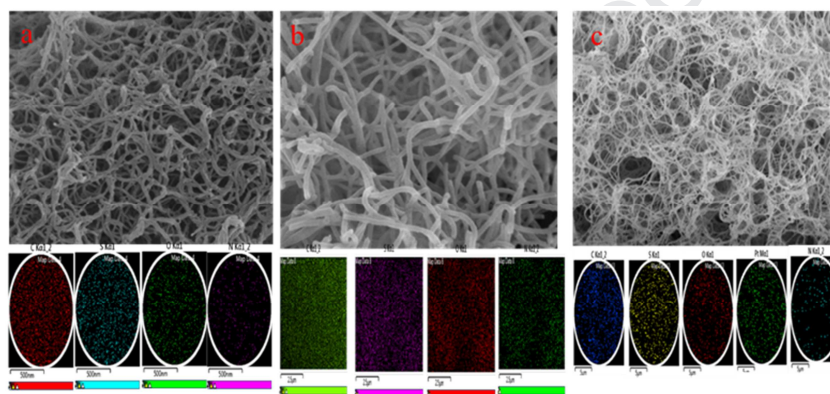


Fig. 4 The SEM images and EDS mapping results of a) $\text{COF-SO}_3\text{H}$, b) $[\text{NH}_4^+][\text{COF-SO}_3^-]$ and c) $\text{Pt}^{\text{I}}@\text{COF}$, respectively.

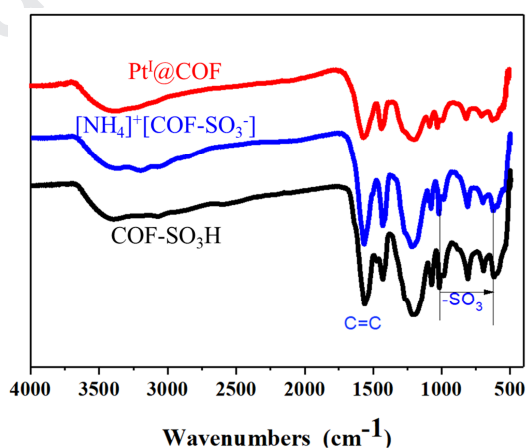
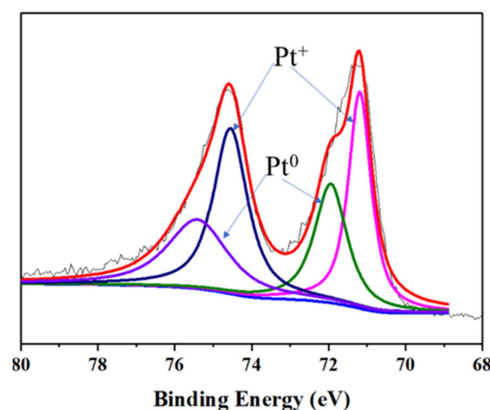


Fig. 5 FT-IR spectra of $\text{COF-SO}_3\text{H}$, $[\text{NH}_4^+][\text{COF-SO}_3^-]$ and $\text{Pt}^{\text{I}}@\text{COF}$.

X-ray photoelectron spectroscopy (XPS) analysis of $\text{Pt}^{\text{I}}@\text{COF}$ was used to probe the chemical valence state of Pt. Quantitative X-ray photoelectron spectroscopy (XPS) (**Fig. 6**) shows that most

1 of the Pt^{2+} atoms have been reduced to Pt^+ after treatment with NaBH_4 , and this value fits better
 2 with that of unsaturated Pt^+ species confined in MOFs[37] or ligated to thiols,[38] which
 3 corresponds to formal Pt^+ rather than to any typical signal for $\text{Pt}(0)$. [39]



4
 5 **Fig. 6** XPS spectra of Pt 4f electrons of $\text{Pt}^{\text{I}}@ \text{COF}$.

6
 7 Compared with $[\text{NH}_4]^+[\text{COF-SO}_3^-]$, the N_2 adsorption capacity at 77 K is largely reduced after
 8 Pt-loaded in sample, giving a BET surface area of $51 \text{ m}^2/\text{g}$, most likely due to the occupation of
 9 pore by Pt nanoparticles (**Fig. 7**). TEM technique was used to characterize the particle sizes of Pt on
 10 $[\text{NH}_4]^+[\text{COF-SO}_3^-]$ (**Fig. 8**). As shown in Fig. 8, $\text{Pt}^{\text{I}}@ \text{COF}$ are still keep the filiform morphology
 11 and Pt NPs uniformly distributed on the surface of material. The average size of Pt NPs in
 12 $\text{Pt}^{\text{I}}@ \text{COF}$ is about 4.6 nm as displayed in Fig.8. The formation of metal NPs, especially for noble
 13 metals, is difficult but important to improve the usage efficiency of expensive metal NPs. The
 14 formation of small Pt clusters on $\text{Pt}^{\text{I}}@ \text{COF}$ is possibly due to the coordination ability of the
 15 sulfonate ligand to Pt NPs. The thermogravimetric analysis (TGA) demonstrates that $\text{Pt}^{\text{I}}@ \text{COF}$
 16 owns excellent thermal stabilities up to 300°C (**Fig. 9**), which provides the demands for potential
 17 applications in catalysis. Inductively coupled plasma (ICP) analysis demonstrates that the Pt content
 18 in the sample is 0.83 wt.%, which is close to that determined by SEM-EDS spectrum (**Table 1**).

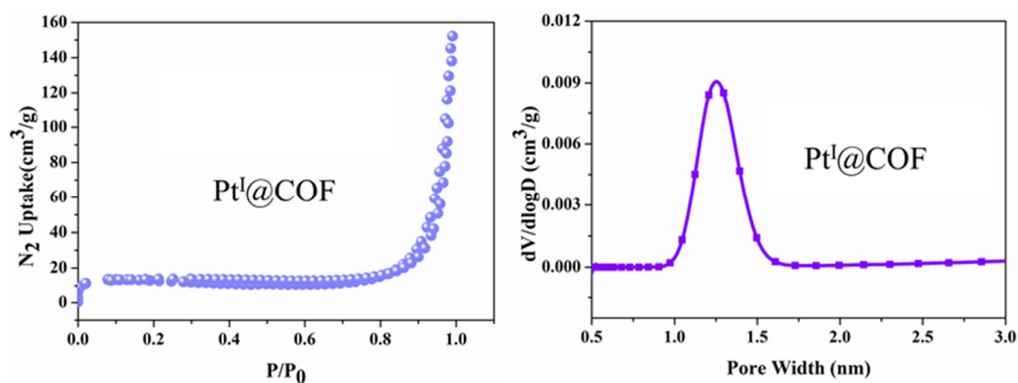


Fig. 7 The N_2 adsorption-desorption at 77K for $Pt^I@COF$ with the insert of distribution of pore size.

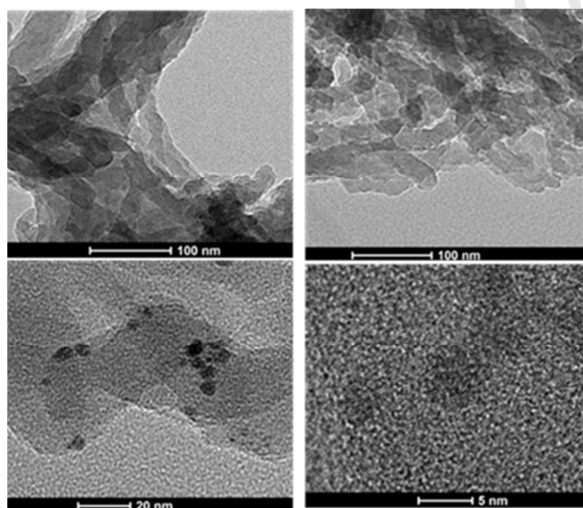


Fig. 8 STEM images of $Pt^I@COF$.

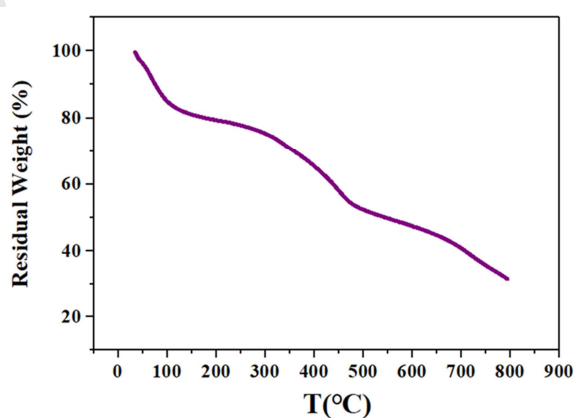


Fig. 9 TGA of $Pt^I@COF$.

Table 1. The element contents of the as- $Pt^I@COF$.

Element	C	N	O	S	Pt	Total
Content(wt.%) ^a	58.86	23.36	12.08	4.87	0.83	100.00
Content(wt.%) ^b	56.75	25.13	11.79	5.42	0.91	100.00

^a determined by element analysis

^b determined by SEM-EDS spectrum

To test the catalytic activity of Pt^I@COF, selective hydrogenation of phenylacetylene was performed. which was carried out with 114 μ L of phenylacetylene, 15.0 mg of the catalyst, and 15 mL of ethanol in a 50mL three-necked round-bottomed flask under controlled H₂ pressures and temperatures. **Fig. 10** shows the conversion of phenylacetylene and selectivity for styrene by the Pt catalysts under the conditions of 1 bar H₂ at different temperature. The Pt^I@COF catalyst afforded 93.5% phenylacetylene conversion and 90.2% styrene selectivity in 20 min, which was apparently the best among the tested temperatures at 25 °C. The kinetic curve of Pt^I@COF indicates that the reaction rate is fast in the initial 20 min without any induction time. Within 40 min, 100% conversion was achieved.

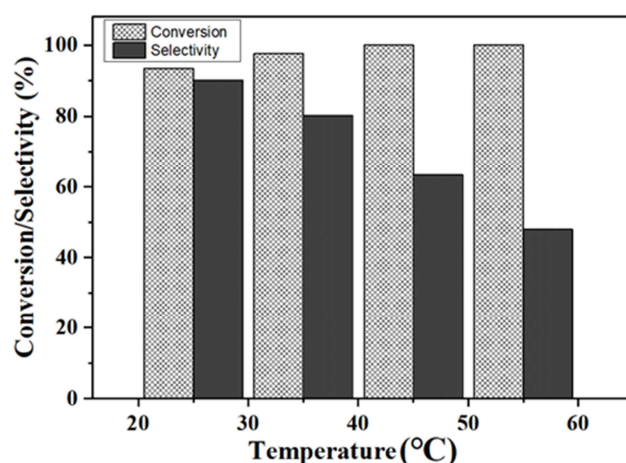


Fig. 10 The conversion of phenylacetylene and selectivity for styrene by Pt^I@COF over the different temperature.

To disclose the catalytic mechanism, a comparison experiments are carried out. Under similar reaction conditions, $\text{Pt}^{2+}@\text{COF}$ (prepared by impregnation of $[\text{Pt}(\text{NH}_3)_4](\text{NO}_3)_2$ on $[\text{NH}_4]^+[\text{COF-SO}_3^-]$ without reduction), $\text{Pt}^0@\text{COF}$ (prepared by spraying method)[40-41] and the pristine $[\text{NH}_4]^+[\text{COF-SO}_3^-]$ were applied to semi-hydrogenation of phenylacetylene. Seen from **Table 2**, Pt including in Pt^{2+} , Pt^+ and Pt^0 shows high catalytic activity for hydrogenation reaction of phenylacetylene. However, only the $\text{Pt}^{\text{I}}@\text{COF}$ catalyst performs high selectivity. Accordingly, Pt^+ loaded on support could be a good candidate for semi-hydrogenation of phenylacetylene. In addition, seen from **Table 3**, by comparing with the reported semi-hydrogenation experiments of alkynes based on Pt catalyst in the literature, it is clearly suggesting that our catalyst presents a highly rare example showing both high selectivity and conversion for semi-hydrogenation. Most importantly, ultrahigh catalytic efficiency for the $\text{Pt}^{\text{I}}@\text{COF}$ catalyst evaluated by the turnover frequency value is up to 3965 h^{-1} , which outperforms most of reported catalysts for such use.

Table 2. Selective hydrogenation of phenylacetylene to styrene on different catalysts.

Catalysts	t (min)	Conversion (%)	Selectivity to styrene (%)
$[\text{NH}_4]^+[\text{COF-SO}_3^-]$	20	2.4	100.0
$\text{Pt}^{2+}@\text{COF}$	72	99.8	8.5
$\text{Pt}^0@\text{COF}$	20	85.8	47.8
$\text{Pt}^{\text{I}}@\text{COF}$	20	93.5	90.2

Table 3. A comparison with other reported catalysts for hydrogenation of alkyne.

Catalyst	$\text{H}_2(\text{bar})$	t(min)	T($^{\circ}\text{C}$)	C(%)	S(%)	TOF(h^{-1})	Ref
$\text{Pt}^{\text{I}}@\text{COF}$	1	20	25	93.5	90.2	3965	This work
Pt/oCNTs	0.4	60	50	98	86	43	17
$\text{Ru}/\text{Pt}/\text{oCNTs}$	0.4	60	50	88	88	132	17
Pt/PSiO_2	20	120	45	99.1	99.5	2304	20
$\text{CN}/\text{Pt}/\text{CNTs}$	0.3	120	50	100	90	812	29
Pt/ZTC	0.5	60	50	63	85	4766	30

MPF-SO ₃ H-Pt	1	15	80	43	89	930	31
Pt	1	550	50	30.8	90.2	1368	32a
Pt/ABSFGF	1	9	51	90	69		32b

The recycling stability of Pt^I@COF was also investigated. As shown in **Fig. 11**, neither conversion nor selectivity exhibited any considerable decrease in comparison with the fresh catalyst. This demonstrates that Pt^I@COF is highly stable and durable. To further confirmation the stability of the sample, the XRD and XPS were detected after 1st cycle and 3rd cycle reaction. From **Fig. 12**, it is demonstrated that the crystalline structure is changed slightly after 1st cycle and 3rd cycle reaction. **Fig. 13** shows that after 1st cycle and 3rd cycle reaction, there is almost no remarkable change of the distribution of Pt NPs in the used Pt^I@COF catalyst. Above results indicate the Pt^I@COF has high stability. Meanwhile, **Fig. 14** shows the change of Pt⁰ of Pt⁰@COF after used. As shown in **Table 4**, it further demonstrates the Pt^I@COF presents excellent catalytic performance under mild reaction conditions for various alkynes, suggesting its superior application in this field.

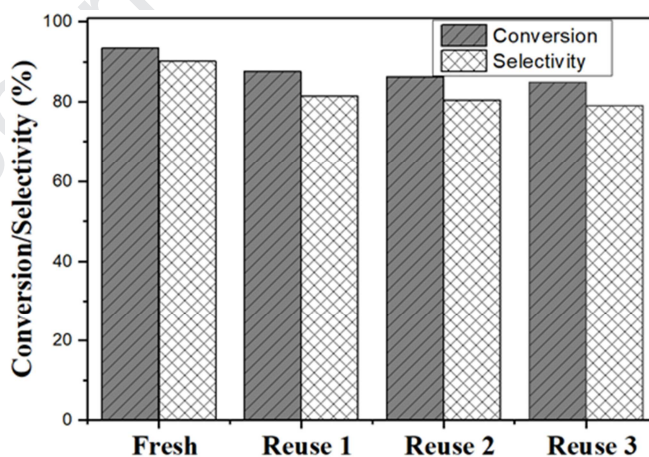


Fig. 11 The recyclability of Pt^I@COF catalyst.

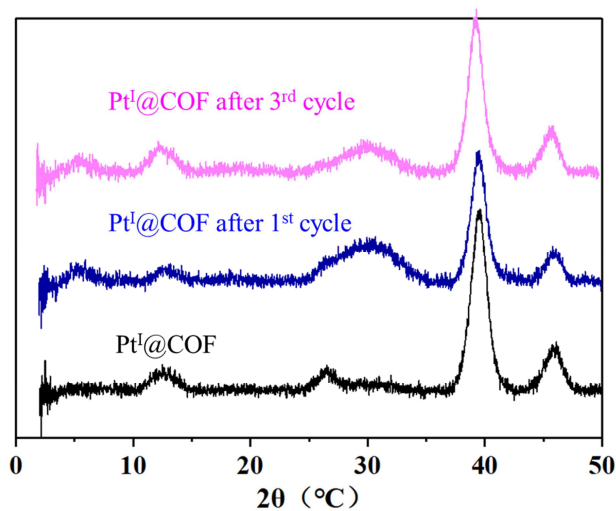


Fig. 12 PXRD patterns of different samples.

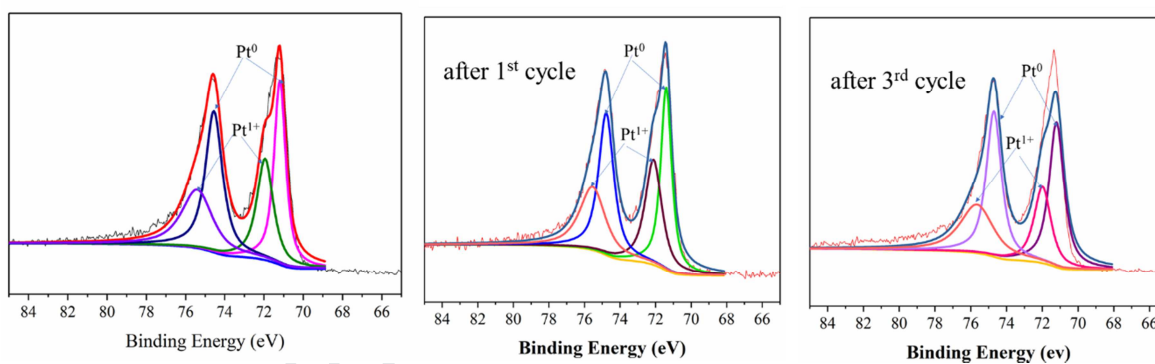


Fig. 13 XPS spectra of different samples for Pt^I@COF.

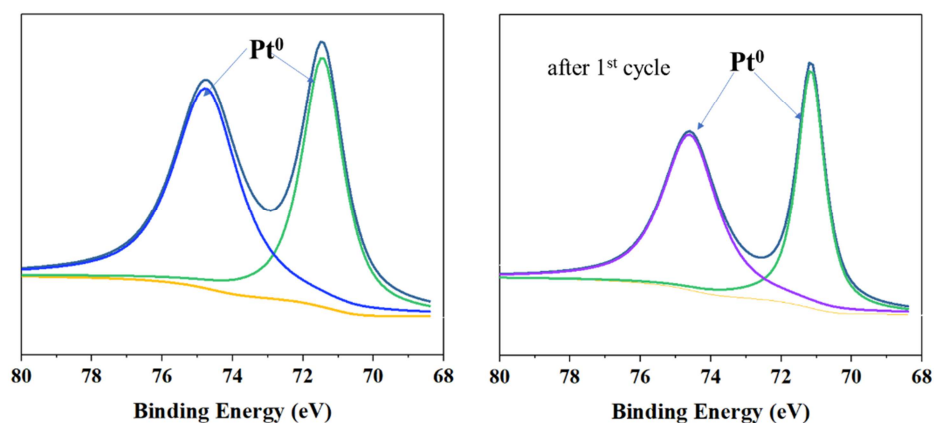
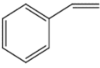
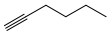
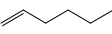
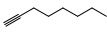
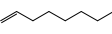

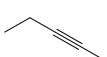


Fig. 14 XPS spectra of different samples for Pt⁰@COF.

Table 4. Semi-hydrogenation of various alkynes catalyzed by Pt^I@COF catalyst.

Entry	Substrate	Time (min)	Product	Conversion (%)	Selectivity (%)
1		20		93.5	90.2
2		120		92.0	89.5
3		80		91.0	90.4
4		25	4-Octene and isomer alkenes	94.0	90.0
5		40	2-pentene and isomer alkenes	92.0	88.7

4. Conclusions

In conclusion, COF-supported catalyst of Pt^I@COF was synthesized by a simple impregnation-reduction method as a novel catalyst for selectively catalyzing hydrogenation of phenylacetylene. It is the first time to prepare the mono-valence Pt^I@COF. And the outstanding catalytic performance is achieved with 93.5% conversion and 90.2% selectivity to styrene under extremely mild reaction conditions (1 bar H₂, 25 °C). Noticeably, the turnover frequency (TOF) value is as high as 3965 h⁻¹, which exceeds most of reported Pt-based catalysts. A series of experimental and characterization results disclose that Pt⁺ on COF can provide not only more accessible active sites for phenylacetylene conversion, but also allow for high selectivity. Moreover, the as-fabricated Pt^I@COF also shows high stability without obvious loss even after three successive runs. This work provides a novel strategy for the fundamental design of COF-supported metal catalysts and thereby provides a new avenue for the fabrication of catalytic materials.

1 **Acknowledgments:**

2 We thanks to the National Science Foundations of China (21871047, 21661001, and
3 U1832148), the Natural Science Foundation of Jiangxi Province of China (20192BAB203002), the
4 Natural Science Foundation of Jiangxi Province of China (20181ACB20003), and the technology
5 program of education department of Jiangxi Province of China (GJJ1505).

8 **Reference**

- 9 [1] T. Vergunst, F. Kapteijn, J. A. Moulijn, Optimization of geometric properties of a monolithic
10 catalyst for the selective hydrogenation of phenylacetylene. *Ind. Eng. Chem.*
11 *Res.*,40(2001)2801-2809.
- 12 [2] J. Xiao, W. Yang, X. H. Chen, Selective Hydrogenation of Phenylacetylene in the Presence
13 of Styrene. *Ind. Catal.*, 12(2004)7-11.
- 14 [3] a)G. Vile', D. Albani, N. Almora-Barrios, N. Lo'pez, and Z. Pe'rez-Ram'irez, Advances in
15 the Design of Nanostructured Catalysts for Selective Hydrogenation. *Chemcatchem.*, 8(2016)
16 21-33.b) X. Zhang, L. Geng, Y. Z. Zhang, D. S. Zhang, R. Zhang, J. Fu, H. Han, Construction
17 of Cu-based MOFs with enhanced hydrogenation performance by integrating open
18 electropositive metal sites. *CrystEngComm.*,36 (2019) 5382-5386.
- 19 [4] D. S. Dominguez, B. A. Murcia, C. D. Amoros, L. A. Solano, Semihydrogenation of
20 phenylacetylene catalyzed by metallic nanoparticles containing noble metals. *J. Catal.*,
21 243(2006) 74-81.
- 22 [5] W. Yu, Z. Xin, S. Niu, T. W. Lin, W. Guo, Y. Xie, Y. Wu, X. Ji, L. Shao, Nanosized
23 palladium on phosphorus-incorporated porous carbon frameworks for enhanced selective
24 phenylacetylene hydrogenation. *Catal. Sci. Technol.*,7 (2017)4934-4939.

- [6] Q. Yang, Q. Xu, H. L. Jiang, Metal–Organic Frameworks Meet Metal Nanoparticles: Synergistic Effect for Enhanced Catalysis. *Chem. Soc. Rev.*, 46(2017) 4774-4808.
- [7] L. Zhu, X. Q. Liu, H. L. Jiang, and L. B. Sun, Metal–Organic Frameworks for Heterogeneous Basic Catalysis. *Chem. Rev.*, 117(2017) 8129-8176.
- [8] a) Z. Gao, F. Q. Liu, L. Wang, F. Luo, Highly Efficient Transfer Hydrodeoxygenation of Vanillin over Sn⁴⁺-induced Highly Dispersed Cu-based Catalyst. *Appl. Surf. Sci.*, 480(2019) 548-556. b) P. Jing, T. Gan, H. Qi, B. Zheng, X. Chu, G. Yu, G. Liu, Synergism of Pt nanoparticles and iron oxide support for chemoselective hydrogenation of nitroarenes under mild conditions. *Chinese Journal of Catalysis.*, 40 (2019) 214-222.
- [9] a) L. X. Yang, H. Q. Wu, H. Y. Gao, J. Q. Li, Y. Tao, W. H. Yin, F. Luo, Hybrid Catalyst of a Metal–Organic Framework, Metal Nanoparticles, and Oxide That Enables Strong Steric Constraint and Metal–Support Interaction for the Highly Effective and Selective Hydrogenation of Cinnamaldehyde. *Inorg. Chem.*, 57(2018) 12461-12465. b) H. Chen, N. Ma, J. Li, Y. Wang, C. She, Y. Zhang, S. Zhou, Effect of atomic iron on hydriding reaction of magnesium: Atomic-substitution and atomic-adsorption cases from a density functional theory study. *Applied Surface Science.*, (2019)144489.
- [10] Y. Tao, H. Q. Wu, J. Q. Li, L. X. Yang, W. H. Yin, M. B. Luo, F. Luo Applying MOF+ Technique for in Situ Preparation of a Hybrid Material for Hydrogenation Reaction. *Dalton Trans.*, 47(2018)14889-14892.
- [11] T. Mitsui, M. K. Rose, E. Fomin, D. F. Ogletree, M. Salmeron, Dissociative Hydrogen Adsorption on Palladium Requires Aggregates of Three or More Vacancies. *Nature.*, 422(2003) 705-707.

- [12] M. M. Dell'Anna, M. Gagliardi, P. Mastrorilli, G. P. Suranna, C. F. Nobile, Hydrogenation Reactions Catalysed by a Supported Palladium Complex. *J. Mol. Catal. A: Chem.C.*, 158(2000)515-520.
- [13] X. Zhang, Z. Wang, S. Li, C. Wang, J. Qiu, Recyclable Catalyst for Catalytic Hydrogenation of Phenylacetylene by Coupling Pd Nanoparticles with Highly Compressible Graphene Aerogels. *RSC Adv.*, 4(2014)59977-59980.
- [14] K. H. Lee, B. Lee, K. R. Lee, M. H. Yi, N. H. Hur, Dual Pd and CuFe₂O₄ Nanoparticles Encapsulated in a Core/Shell Silica Microsphere for Selective Hydrogenation of Arylacetylenes. *Chem. Commun.*, 48(2012) 4414-4416.
- [15] T. Yoshii, K. Nakatsuka, Y. Kuwahara, K. Mori, and H. Yamashita, Synthesis of CarbonSupported Pd–Co Bimetallic Catalysts Templated by Co Nanoparticles Using the Galvanic Replacement Method for Selective Hydrogenation. *RSC Adv.*, 7(2017)22294-22300.
- [16] J. Liu, Y. N. Zhu, C. Liu, X. S. Liu, C. Y. Cao, and W. G. Song, Excellent Selectivity with High Conversion in Semi-Hydrogenation of Alkynes Using Pd-based Bimetallic Catalysts. *ChemCatChem.*, (2017) 1-6.
- [17] D. Deng, Y. Yang, Y. Gong, Y. Li, X. Xu, Y. Wang, Palladium Nanoparticles Supported on mpg-C₃N₄ as Active Catalyst for Semihydrogenation of Phenylacetylene under Mild Conditions. *Green Chem.*, 15(2013) 2525-2531.
- [18] D. Bhuyan, K. Selvaraj, L. Saikia, Pd@SBA-15 Nanocomposite Catalyst: Synthesis and Efficient Solvent-free Semihydrogenation of Phenylacetylene under Mild Conditions. *Microporous Mesoporous Mater.*, 241(2017) 266-273.

- [19] H. Zhou, X. Yang, L. Li, X. Liu, Y. Huang, X. Pan, A. Wang, J. Li, T. Zhang, PdZn Intermetallic Nanostructure with Pd–Zn–Pd Nanoparticles for Highly Active and Chemoselective Semi-hydrogenation of Acetylene. *ACS. Catal.*, 6(2016) 1054-1061.
- [20] S. Mandal, D. Roy, R.V. Chaudhari, M. Sastry, Pt and Pd Nanoparticles Immobilized on Amine-functionalized Zeolite: Excellent Catalysts for Hydrogenation and Heck Reactions. *Chem. Mater.*, 16(2004) 3714-3724.
- [21] L. Shen, S. Mao, J. Li, M. Li, P. Chen, H. Li, Z. Chen, Y. Wang, PdZn Intermetallic on a CN@ZnO Hybrid as an Efficient Catalyst for the Semi-hydrogenation of Alkynols. *J.Catal.*, 350(2017) 13-20.
- [22] M. Z. Hu, J. Zhang, W. Zhu, Z. Chen, X. Gao, X. J. Du, J. W. Wan, K. B. Zhou, C. Chen and Y. D. Li, 50 ppm of Pd Dispersed on Ni(OH)₂ Nanosheets Catalyzing Semi-hydrogenation of Acetylene with High Activity and Selectivity. *Nano Res.*, 11(2018)905-912.
- [23] J. Deng, P. Ren, D. Deng, X. Bao, Enhanced Electron Penetration Through an Ultrathin Graphene Layer for Highly Efficient Catalysis of the Hydrogen Evolution Reaction. *Angew. Chem. Int. Ed.*, 54(2015) 2100-2104.
- [24] H. Liu, L. Zhang, N. Wang, D. S. Su, Palladium Nanoparticles Embedded in the Inner Surfaces of Carbon Nanotubes: Synthesis, Catalytic Activity, and Sinter Resistance. *Angew. Chem. Int. Ed.* 53(2014) 12634-12638.
- [25] H. Q. Wu, L. Huang, J. Q. Li, A. M. Zheng, Y. Tao, L. X. Yang, W. H. Yin and F. Luo, Pd@Zn-MOF-74: Restricting a Guest Molecule by the Open-Metal Site in a Metal–Organic Framework for Selective Semihydrogenation. *Inorg. Chem.*, 57(2018)12444-12447.
- [26] a) C. Li, Z. Shao, M. Pang, C. T. Williams, C. Liang, Carbon Nanotubes Supported Pt

- 1 Catalysts for Phenylacetylene Hydrogenation: Effects of Oxygen Containing Surface Groups
2 on Pt Dispersion and Catalytic Performance. *Catal. Today.*, 186(2012) 69-75. b) X. Zhang, N.
3 Wang, L. Geng, J. Fu, H. Hu, D. Zhang, H. Han, Facile synthesis of ultrafine cobalt oxides
4 embedded into N-doped carbon with superior activity in hydrogenation of 4-nitrophenol. *Journal of*
5 *colloid and interface science.*, 512(2018) 844-852.c) H. Chen, J. Liu, P. Liu, Y. Wang, H. Xiao, Q.
6 Yang, S. Zhou, Carbon-confined magnesium hydride nano-lamellae for catalytic hydrogenation of
7 carbon dioxide to lower olefins. *Journal of Catalysis.*, 379(2019) 121-128.
- 8 [27] a) C. Li, Z. Shao, M. Pang, C. T. Williams, X. Zhang, C. Liang, Carbon Nanotubes
9 Supported Mono- and Bimetallic Pt and Ru Catalysts for Selective Hydrogenation of
10 Phenylacetylene. *Ind. Eng. Chem. Res.*, 51(2012) 4934-4941. b) N. Zhang, X. Wang, L. Geng, Z.
11 Liu, X. Zhang, C. Li, G. Zhao, Metallic Ni nanoparticles embedded in hierarchical mesoporous Ni
12 (OH) 2: A robust and magnetic recyclable catalyst for hydrogenation of 4-nitrophenol under mild
13 conditions[J]. *Polyhedron.*, 164(2019) 7-12.
- 14 [28] S. Jayakumar, A. Modak, M. Guo, H. Li, X. P. Hu, Q. H. Yang, Ultrasmall Platinum
15 Stabilized on Triphenylphosphine-modified Silica for Chemoselective Hydrogenation. *Chem.*
16 *Eur. J.*, 23(2017) 7791-7797.
- 17 [29] I. F. Jaffe, A. Efraty, New Palladium(0) Platinum(0) 4,4'-Diisocyanobiphenyl Matrices for
18 Heterogeneous Catalytic Hydrogenation of Alkenes and Alkynes. *J. Mol. Catal.*,
19 35(1986)285-302.
- 20 [30] C. X. Jiang, K. Hara, K. Namba, H. Kobayashi, S. Ittisanronnachai, H. Nishihara, T.
21 Kyotani, A. Fukuoka, Preparation of Highly Dispersed Pt Nanoparticles Supported on
22 Zeolite-templated Carbon and Catalytic Application in Hydrogenation Reaction. *Chem. Lett.*,
23 43(2014) 1794-1796.

- [31] A. P. Cote, A. I. Benin, N. W. Ockwig, M. O'keefe, A. J. Matzger, O. M. Yaghi, Porous, Crystalline, Covalent Organic Frameworks. *Sci.*, 310(2005) 1166–1170.
- [32] a) S. S. Yuan, X. Li, J. Y. Zhu, G. Zhang, P. V. Puyvelde, and B. V. D. Bruggen, Covalent Organic Frameworks for Membrane Separation. *Chem. Soc. Rev.*, 48(2019)2665-2681. b) V. G. Dorokhova, N. V. Bykovaa, M. V. Kuznetsovb, L. A. Bykovc, and V. V. Barelko, Study of Pyridine-Modified Platinum and Palladium-containing Selective-Hydrogenation Catalysts on Fiber-Glass Woven Support. *Russian Journal of Applied Chemistry.*, 89(2016)1769–1776.
- [33] X. H. Xiong, Z. W. Yu, L. L. Gong, Y. Tao, Z. Gao, L. Wang, W. H. Yin, L. X. Yang, F. Luo, Ammoniating Covalent Organic Framework (COF) for High-Performance and Selective Extraction of Toxic and Radioactive Uranium Ions. *Adv. Sci.*, 6(2019)1900547.
- [34] Y. Tao, R. Krishna, L. X. Yang, Y. L. Fan, L. Wang, Z. Gao, J. B. Xiong, L. J. Sun, F. Luo, Enhancing C₂H₂/C₂H₄ separation by incorporating low-content sodium in covalent organic frameworks. *Inorg. Chem. Front.*, 6(2019) 2921-2926.
- [35] F. Kakiuchi, S. Takano, T. Kochi, Catalytic Reactions of Terminal Alkynes Using Rhodium(I) Complexes Bearing 8-Quinolinolate Ligands. *ACS Catal.*, 8(2018) 6127-6137.
- [36] J. H. Chong, M. Sauer, B. O. Patrick and M. J. MacLachlan, Highly Stable Keto-enamine Salicylideneanilines. *Org. Lett.*, 5(2003) 3823-3826.
- [37] R. Vakili, E. K. Gibson, S. Chansai, S. Xu, N. Al-Janabi, P. P. Wells, C. Hardacre, A. Walton, X. Fan, Understanding the CO Oxidation on Pt Nanoparticles Supported on MOFs by Operando XPS. *ChemCatChem.*, 10(2018) 4238-4242.
- [38] X. Fu, Y. Wang, N. Wu, L. Gui, Y. Tang, Surface Modification of Small Platinum Nanoclusters with Alkylamine and Alkylthiol: An XPS Study on the Influence of Organic

- 1 Ligands on the Pt 4f Binding Energies of Small Platinum Nanoclusters. *J. Col. Interf. Sci.*,
2 243(2001)326-330.
- 3 [39] J. R. Reimers, M. J. Ford, A. Halder, J. Ulstrup, N. S. Hush, Proceed Gold Surfaces and
4 Nanoparticles are Protected by Au(0)-thiyl Species and are Destroyed When Au(I)-Thiolates
5 Form. *Nat. Am. Soc.*, 113(2016) 1424-1433.
- 6 [40] J. H. Li, L. X. Yang, J. Q. Li, W. H. Yin, Y. Tao, H. Q. Wu, F. Luo, Anchoring nZVI on
7 metal-organic framework for removal of uranium(\square) from aqueous solution. *J. Solid State*
8 *Chem.*, 269(2019) 16-23.
- 9 [41] Y. Y. Xiong, J. Q. Li, C. S. Yan, H. Y. Gao, J. P. Zhou, L. L. Gong, M. B. Luo, L. Zhang,
10 P. P. Meng, F. Luo, MOF catalysis of FeII-to-FeIII reaction for an ultrafast and one-step
11 generation of the Fe₂O₃@MOF composite and uranium(VI) reduction by iron(II) under
12 ambient conditions. *Chem. Commun.*, 52(2016) 9538-9541.
- 13 [42] L. X. Xia, D. Li, J. Long, F. Huang, L. N. Yang, Y. S. Guo, Z. M. Jia, J. P. Xiao, H. Y.
14 Liu, N-doped graphene confined Pt nanoparticles for efficient semi- hydrogenation of
15 phenylacetylene. *Carbon.*, 145(2019) 47-52.
- 16 [43] S. Galvagno, Z. Poltarzewski, A. Donato, G. Neri, R. Pietropaolo, Liquid phase
17 hydrogenation over platinum-tin catalysts. *J. Mol. Catal. A: Chem.*, 35(1986) 366-373.
- 18 [44] M. P. Boronoev, E. S. Subbotina, A. A. Kurmaeva, Y. S. Kardasheva, A. L. Maksimov, E.
19 A. Karakhanov, Platinum and palladium nanoparticles in modified mesoporous phenol–
20 formaldehyde polymers as hydrogenation catalysts. *Petrol. Chem.*, 56(2016)109-120.
- 21 [45] S. D. Domínguez, Á. B. Murcia, D. C. Amorós, Á. L. Solano, Semihydrogenation of
22 phenylacetylene catalyzed by metallic nanoparticles containing noble metals. *J. Catal.*,
23 243(2006) 74-81.

Highlights:

1. This work presents the first case of mono-valence Pt^{I} @COF for semi-hydrogenation reactions of phenylacetylene.
2. This work firstly present a simple impregnation-reduction method for the preparation of Pt-anchored covalent organic framework (Pt^{I} @COF).
3. Pt^+ and Pt^0 can synergistically promote the transformation of phenylacetylene to styrene.
4. The Pt^{I} @COF exhibits remarkable performance with 93.5% conversion and 90.2% selectivity to styrene under mild reaction conditions (1 bar H_2 , 25 °C).
5. This kind of material is highly repeatable for such use.

Declaration of interests

☐ The authors declare that they have no known competing financial interests or personal relationships that could have appeared to influence the work reported in this paper.

☒ The authors declare the following financial interests/personal relationships which may be considered as potential competing interests: